MAGNETIC FIELD RECONSTRUCTION FROM SPARSE MEASUREMENTS FOR COMPLEX GEOMETRIES*

J. W. Phillips†, B. Naranjo, J. B. Rosenzweig
University of California Los Angeles, United States
P. Alva Rosa, Augsburg University, Minneapolis, United States
J. A. Phillips, MiraCosta College, Oceanside, United States
D. McCormick, D. Storey, J. M. Cruz Jr.
SLAC National Accelerator Laboratory, Menlo Park United States

Abstract

Precise 3D field measurements of large, complex magnet geometries are time-consuming and error-susceptible. For large magnets, it is common to record Hall probe data on a sparse grid, then use an interpolation algorithm to estimate field values at the remaining points. For common magnet geometries, such as quadrupoles and dipoles, linear interpolation often provides accurate results. However, for complex magnet geometries, this method can yield lower accuracy. In this paper, we present a method based on a locally Maxwell-consistent algorithm for sparse Hall probe measurements. Through the k-nearest neighbors algorithm, we locally fit the magnetic field with Tikhonov regularization. We test this method on a novel Compton spectrometer, capable of measuring single-shot, double-differential, energy-angle gamma spectra, ranging from 180 keV to 28 MeV. Using held-out validation, we demonstrate that we can reconstruct its magnetic fields with higher accuracy than linear interpolation and radial basis function (RBF) interpolation with cubic, thin plate spline, and quintic kernels. We also analyze the dependence of point sparsity on accuracy.

INTRODUCTION

Magnets are ubiquitous in particle accelerators, serving to focus beams, correct aberrations, and analyze particle energies. Precise field characterization is essential for beam-transport simulations and magnet evaluation [1]. Common methods of characterizing magnetic fields are Hall probe and rotating coil measurements [2]. These procedures take long periods of time, limiting grid fineness over large volumes; the magnetic field must then be reconstructed in the regions between the measured points through interpolation. For conventional magnet geometries with dominant multipole fields, there exist analytic models that can be used for a full 3D reconstruction [3]. Achieving an accurate reconstruction through global fitting can be difficult, however, for complex geometries. Alternatively, common interpolation methods like linear and radial basis function (RBF) interpolation can be used; however, they do not automatically enforce Maxwell's equations, resulting in potentially non-physical results. There exist more sophisticated methods that enforce Maxwell's equations, including Gaussian process regression with Maxwell-consistent kernels [4, 5], utilization of a harmonic basis [6–8], and other divergence-free approaches [9–11]. However, each of these methods is limited by computational expense, regular grid requirements, incomplete Maxwell enforcement, or incompatibility with Hall probe measurements.

* The authors thank the Tigner Traineeship in Accelerator Science, DOE award DE-SC0024907, and the US Department of Energy, under Contract No. DE-SC0009914.
† jphillips@physics.ucla.edu

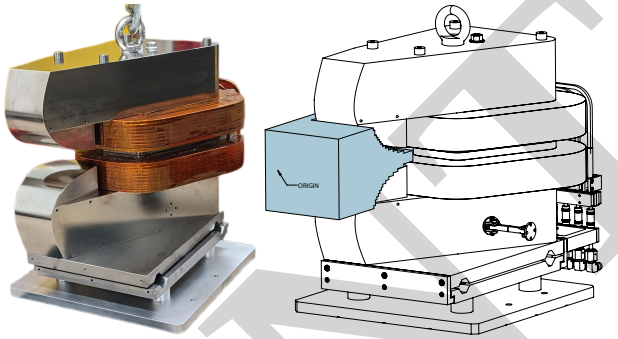

Figure 1: The left image shows CPT, the gamma spectrometer built at UCLA. The filled-in region on the right drawing illustrates the magnetic field measurement volume.

At the University of California, Los Angeles (UCLA), we are building a broadband Compton spectrometer, dubbed CPT, for installation at FACET-II SLAC National Laboratory as shown in Fig. 1 [12–14]. Its complex geometry requires a precise 3D field map, motivating our development of a simple yet accurate method for magnetic field reconstruction that is effective on sparse measurements. We find the nearest k points using a k-nearest neighbors (KNN) search. We then use Tikhonov regularized least squares to locally fit a harmonic polynomial expansion to the measured field values in that neighborhood. Since the harmonic polynomial basis functions are solutions to Laplace's equation by construction, the reconstructed field is locally Maxwell-consistent.

Using held-out validation, we apply this method to Hall probe measurements of CPT. Next, we compare to linear and RBF interpolation with various kernels. We then demonstrate how the interpolation accuracy degrades with sparsity.

A NOVEL COMPTON SPECTROMETER

CPT is a single-shot, double-differential, energy-angle gamma spectrometer capable of measuring energy from 180 keV to 28 MeV. Incident photons Compton scatter off a beryllium wire, resulting in Compton electrons. These elec-

trons are subsequently bent with a sextupole-like field into a scintillating screen. For the electron trajectories in this field, the length is proportional to the cube root of momentum, hence allowing for a very broadband measurement of energy. Because electrons of different energies and emission angles traverse distinct trajectories throughout the full magnet volume, accurate particle tracking requires knowledge of the magnetic field in the entire 3D volume rather than along a single reference trajectory. Hall probe measurements on CPT with a 10 mm grid took about nine hours in the region shown in Fig. 1. Measurements on a 1 mm grid would take up to 1,000 times longer, necessitating field reconstruction.

ALGORITHM DESCRIPTION

Current-free Maxwell Constraints

Due to the region of interest being current-free, Maxwell's equations for the magnetic field $\mathbf{B}$ reduce to

$$\begin{aligned} \nabla \times \mathbf{B} = 0 \quad &\Longrightarrow \quad \mathbf{B} = -\nabla \Phi \\ \nabla \cdot \mathbf{B} = 0 \quad &\Longrightarrow \quad \nabla^2 \Phi = 0, \end{aligned}$$

where the zero curl implies the magnetic field is the gradient of a scalar function Φ. Combined with the zero divergence, this scalar potential will be harmonic.

For our reconstruction, we choose a harmonic basis and fit its gradient to the magnetic field data. By doing this, we ensure that it is Maxwell-consistent and requires fewer fitting parameters. This allows for greater efficiency compared to interpolating each magnetic field component independently, while keeping the reconstruction physics-constrained.

Harmonic Polynomials

For our basis, we use harmonic polynomials—polynomials that obey Laplace's equation—generated with a formula found by E.P. Miles, Jr. and Ernest Williams [15,16]. Polynomials allow us to readily reconstruct systems without symmetry while being one of the most computationally efficient functions.

Interpolation

Given a list of to-be-interpolated query points and a list of magnetic field measurements, we iterate through each query point, applying a KNN search to find the nearest k measurement points. For the KNN search, we normalize the points by the range along each axis. This generates a neighborhood $\mathcal{N}_q$ uniquely corresponding to each query point $\mathbf{x}_q$. With k points and N basis functions, we then construct the matrix $\mathbf{A}_q \in \mathbb{R}^{3k\times N}$,

$$\mathbf{A}_q = \begin{pmatrix} \partial_x H_1(\tilde{\mathbf{x}}_1) & \partial_x H_2(\tilde{\mathbf{x}}_1) & \cdots & \partial_x H_N(\tilde{\mathbf{x}}_1) \\ \partial_y H_1(\tilde{\mathbf{x}}_1) & \partial_y H_2(\tilde{\mathbf{x}}_1) & \cdots & \partial_y H_N(\tilde{\mathbf{x}}_1) \\ \partial_z H_1(\tilde{\mathbf{x}}_1) & \partial_z H_2(\tilde{\mathbf{x}}_1) & \cdots & \partial_z H_N(\tilde{\mathbf{x}}_1) \\ \vdots & & & \vdots \\ \partial_z H_1(\tilde{\mathbf{x}}_k) & \cdots & & \partial_z H_N(\tilde{\mathbf{x}}_k) \end{pmatrix}, \quad (1)$$

where ∂_{x_i} is shorthand notation for $\partial/\partial x_i$ with i being an arbitrary integer between 1 and k. H_n is the n-th harmonic basis function and $\tilde{\mathbf{x}}_i = \mathbf{x}_i/r_0$ are the coordinates of the i-th neighbor normalized by the local scale $r_0 = \max_{\mathcal{N}_q} \|\mathbf{x}_i\|$, hence finding the maximum l2-norm over $\mathcal{N}_q$.

With Tikhonov regularization, we solve [17]

$$\mathbf{c}_q = \left(\mathbf{A}_q^\top \mathbf{A}_q + \lambda \mathbf{I}\right)^{-1} \mathbf{A}_q^\top \mathbf{b}_q, \quad (2)$$

where $\mathbf{b}_q = [B_x(\tilde{\mathbf{x}}_1), B_y(\tilde{\mathbf{x}}_1), B_z(\tilde{\mathbf{x}}_1), \ldots, B_z(\tilde{\mathbf{x}}_K)]^\top$ are the measured field values for each $\mathbf{x}_i \in \mathcal{N}_q$. Additionally, $\mathbf{c}_q \in \mathbb{R}^N$ is the optimized harmonic polynomial coefficients. $\mathbf{I} \in \mathbb{R}^{N\times N}$ is the identity matrix and λ is the Tikhonov regularization parameter. Finally, we use the $\mathbf{c}_q$ to predict the field at query point $\mathbf{x}_q$ with

$$\mathbf{B}(\mathbf{x}_q) = \mathbf{A}'_q \mathbf{c}_q, \qquad \mathbf{A}'_q \in \mathbb{R}^{3\times N}, \quad (3)$$

where $\mathbf{A}'_q$ is Eq. 1 and $\mathbf{x}_q$ is the only point in the neighborhood $\mathcal{N}_q$.

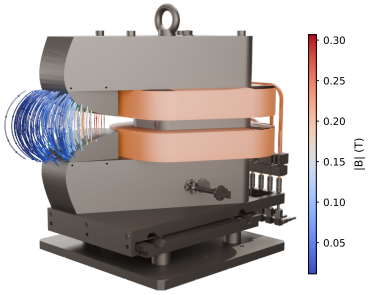

Figure 2: Streamline plot of the CPT magnetic field at 60 A.

CPT RECONSTRUCTION TESTS

Magnetic field measurements described in Fig. 1 were taken at various currents. For our reconstruction, we use the 60 A measurements, shown in Fig. 2. For the tests, we split the measured magnetic field into a training set and testing set by taking every other point in the list of positions, resulting in 2,485 training points and 2,484 held-out test points. We apply our local harmonic algorithm with $N = 45$, $k = 15$, and $\lambda = 10^{-11}$. We then perform the same reconstruction using linear interpolation and RBF interpolation with linear, cubic, thin plate spline, and quintic kernels for comparison. The per-component reconstruction error $\epsilon_i^{(c)}$ is defined as

$$\epsilon_i^{(c)} = |B_i^{\text{pred}} - B_i^{\text{true}}|, \quad (4)$$

for $i = x, y, z$. From this, we define the per-point error as $\epsilon_i^{(p)} = \epsilon_x^{(c)} + \epsilon_y^{(c)} + \epsilon_z^{(c)}$. We likewise define the total error $\epsilon^{(t)}$ as the sum of the per-point error over all points.

To evaluate how sparsity affects accuracy, we perform the same analysis, taking every nth point (1/2 to 1/10th) and reconstructing the remaining points.

RESULTS

CPT Reconstruction

Figure 3 compares the reconstructed and measured magnetic field magnitudes. Table 1 summarizes the reconstruction accuracy. Our local harmonic interpolation method

Table 1: Summary of reconstruction results. The mean, median, and max error are computed over all per-component errors defined in Eq. 4; the total error is their sum. Percentile columns p50–p95 report per-point reconstruction error for the 50th to 95th percentiles. Bold entries indicate the best-performing method for each metric.

Method	Total error (T)	Mean (mT)	Median (mT)	Max (mT)	p50 (mT)	p75 (mT)	p95 (mT)
Local harmonic	**1.04**	**0.14**	**0.007**	**30.1**	0.024	**0.074**	**1.520**
Linear	5.28	0.71	0.142	60.0	0.557	1.434	8.603
RBF linear	3.30	0.44	0.008	53.5	0.032	0.343	6.282
RBF cubic	3.44	0.46	0.061	59.6	0.229	0.676	6.093
RBF thin plate spline	2.67	0.36	**0.007**	50.2	**0.022**	0.400	5.084
RBF quintic	2.71	0.36	0.014	46.7	0.064	0.655	4.883

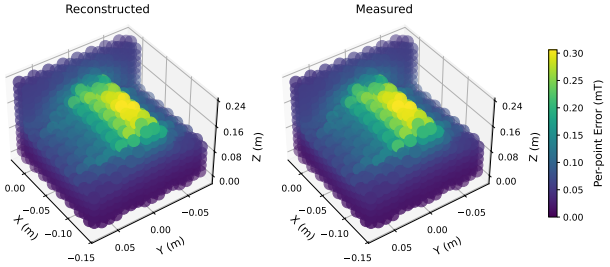

Figure 3: The left column shows the algorithm applied to half of the 4,969 measured points when trained on the remaining half. The right column plots the actual, measured fields.

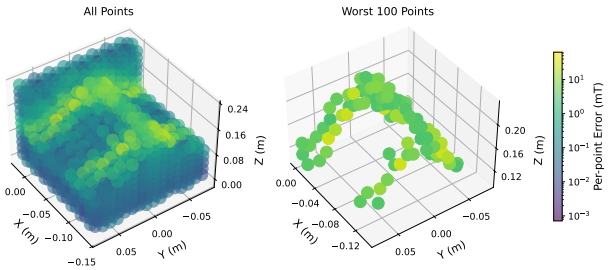

Figure 4: Above is the spatial distribution of per-point error, along with the worst 100 points, shown on a log scale.

achieves a total error of 1.04 T, which is 5.1 times better than linear interpolation and 2.6 times better than the best RBF interpolation, which used a thin plate spline kernel. For the median error, it achieves an error of 7 µT, which is 20.3 times better than linear interpolation. RBF with a thin plate spline kernel has a similar median to local harmonic. However, local harmonic outperforms all other methods on mean error, with a value of 14 µT.

The local harmonic method also achieves lower error from p75 to p95. At p50, RBF thin plate spline achieves 0.022 mT, slightly outperforming the local harmonic error of 0.024 mT; however, at p95, the local harmonic method achieves 1.520 mT compared to 4.883 mT for the best RBF method, a factor of 3.2 improvement. The local harmonic's ability to outperform other methods at higher percentiles reflects a physics-constrained method's ability to better represent fringe points. Throughout all metrics, linear interpolation performs the worst, demonstrating its limitations.

Figure 4 shows the spatial distribution of reconstruction errors. High-error points are in the fringe field regions at

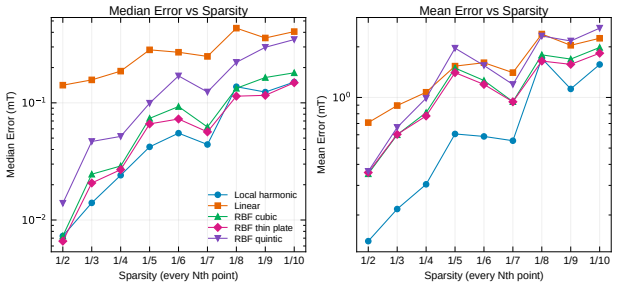

Figure 5: The left plot is a sparsity comparison of the median error, and the right plot is a comparison of the mean.

the magnet boundaries and near the coils, consistent with the rapidly varying field structure in that region.

Sparsity Comparison

Figure 5 shows the median and mean per-point reconstruction error as a function of measurement sparsity for all methods. The local harmonic consistently performs as one of the lowest error methods. This is more pronounced for the mean, which is due to better handling of the fringe fields compared to the other approaches. All methods degrade when they have access to fewer points. From 1/2 to 1/10th sparsity, linear interpolation degrades from a mean per-point error of 0.71 mT to 2.25 mT. Local harmonic, on the other hand, degrades from 0.14 mT to 1.57 mT.

CONCLUSION

We have presented a locally Maxwell-consistent method for reconstructing 3D magnetic fields from sparse Hall probe measurements, based on k-nearest neighbor search and Tikhonov-regularized harmonic polynomial fitting. Applied to Hall probe measurements of a novel Compton spectrometer, the method achieves a median reconstruction error of 7 µT. Furthermore, its total error outperforms linear interpolation by a factor of 5.1 and RBF methods by a factor of 2.6. At all percentiles, from p75 to p95, the local harmonic method outperforms all other approaches, demonstrating its ability to better reconstruct fringe regions. A sparsity sweep from 1/2 to 1/10 of available measurements shows that all methods consistently degrade in accuracy, with RBF and local harmonic methods massively outperforming linear interpolation. Future work will extend this method to additional magnet geometries and investigate noise filtering.

REFERENCES

[1] B. Auchmann, S. Kurz, C. Petrone, and S. Russenschuck, "Generalized harmonic analysis of computed and measured magnetic fields," *IEEE Trans. Magn.*, vol. 52, no. 3, pp. 1–4, Mar. 2016, Art. no. 8000704. doi:10.1109/TMAG.2015.2478336

[2] M. Lopes, "Magnetic measurements," US Particle Accelerator School, Austin, TX, USA, Jan. 2016. https://uspas.fnal.gov/materials/16Austin/lecture06.pdf

[3] B. D. Muratori, J. K. Jones, and A. Wolski, "Analytical expressions for fringe fields in multipole magnets," *Phys. Rev. ST Accel. Beams*, vol. 18, p. 064001, Jun. 2015. doi:10.1103/PhysRevSTAB.18.064001

[4] A. Solin, M. Kok, N. Wahlström, T. B. Schön, and S. Särkkä, "Modeling and interpolation of the ambient magnetic field by Gaussian processes," *IEEE Trans. Robot.*, vol. 34, no. 4, pp. 1112–1127, Aug. 2018. doi:10.1109/TRO.2018.2830326

[5] N. Wahlström, M. Kok, T. B. Schön, and F. Gustafsson, "Modeling magnetic fields using Gaussian processes," in *Proc. IEEE Int. Conf. Acoustics, Speech and Signal Processing (ICASSP)*, Vancouver, BC, Canada, May 2013, pp. 3522–3526. doi:10.1109/ICASSP.2013.6638313

[6] I. G. Ion *et al.*, "Local field reconstruction from rotating coil measurements in particle accelerator magnets," *Nucl. Instrum. Methods Phys. Res. A*, vol. 1011, p. 165580, 2021. doi:10.1016/j.nima.2021.165580

[7] G. T. Bodwin, H. S. Chung, and J. Repond, "Implementation of Maxwell's equations in the reconstruction of the magnetic field in the $g-2$ storage ring," *J. Instrum.*, vol. 14, p. P07002, Jul. 2019. doi:10.1088/1748-0221/14/07/P07002

[8] J. L. R. Ramon, "Maxwellian interpolation of magnetic fields on a grid," B.Sc. thesis, Dept. of Applied Physics, University of Groningen, Groningen, The Netherlands, 2018. https://fse.studenttheses.ub.rug.nl/17945/

[9] O. Beznosov, J. Bonilla, X.-Z. Tang, and G. A. Wimmer, "High order interpolation of magnetic fields with vector potential reconstruction for particle simulations," *Comput. Phys. Commun.*, vol. 316, p. 109770, Jul. 2025. doi:10.1016/j.cpc.2025.109770

[10] R. B. Torbert *et al.*, "A new method of 3-D magnetic field reconstruction," *Geophys. Res. Lett.*, vol. 47, no. 3, p. e2019GL085542, Feb. 2020. doi:10.1029/2019GL085542

[11] M. Yang, D. del-Castillo-Negrete, G. Zhang, and M. T. Beidler, "A divergence-free constrained magnetic field interpolation method for scattered data," *Phys. Plasmas*, vol. 30, p. 033901, Mar. 2023. doi:10.1063/5.0138905

[12] B. Naranjo, "Gamma detection: Compton and pair spectrometers," presented at FACET-II User Meeting, SLAC National Accelerator Laboratory, Menlo Park, CA, USA, Oct. 2023. https://facet-ii.slac.stanford.edu/sites/default/files/2024-01/Gamma%20Detection%20Compton%20and%20Pair%20Spectrometers_Brian%20Naranjo.pdf

[13] B. Naranjo *et al.*, "Compton Spectrometer for FACET-II", in *Proc. IPAC'21*, Campinas, Brazil, May 2021, pp. 4332–4335. doi:10.18429/JACoW-IPAC2021-THPAB269

[14] M. Yadav, *et al.*, "Reconstruction of beam parameters and betatron radiation spectra measured with a Compton spectrometer," *Phys. Rev. Accel. Beams*, vol. 28, p. 042802, Apr. 2025. doi:10.1103/PhysRevAccelBeams.28.042802

[15] E. P. Miles, Jr. and E. Williams, "A basic set of homogeneous harmonic polynomials in k variables," *Proc. Am. Math. Soc.*, vol. 6, no. 2, pp. 191–194, Apr. 1955. doi:10.2307/2032337

[16] A. Urintsev, "Basic sets of polynomial solutions for the iterated Laplace and wave equations," Wolfram MathSource, 1991, http://library.wolfram.com/infocenter/MathSource/3203/

[17] A. N. Tikhonov, "Solution of incorrectly formulated problems and the regularization method," *Soviet Math. Dokl.*, vol. 4, pp. 1035–1038, 1963.